Proceedings of Symposia in Applied Mathematics

Non-oscillatory Central Schemes for 3D Hyperbolic Conservation Laws

Jorge Balbás and Xin Qian

Abstract. We present a family of high-resolution, semi-discrete central schemes for hyperbolic systems of conservation laws in three space dimensions. The proposed schemes require minimal characteristic information to approximate the solutions of hyperbolic conservation laws, resulting in simple *black box* type solvers. Along with a description of the schemes and an overview of their implementation, we present numerical simulation of a cloud-shock interaction modeled by Euler equations of gas dynamics. This demonstrates the versatility and robustness of the semi-discrete central formulation for solving hyperbolic models.

1. Introduction

In this paper we present a new family of high-resolution central schemes for hyperbolic conservation laws and related time dependent problems. We are interested in hyperbolic PDEs of the form

$$u_t + f(u)_x + g(u)_y + h(u)_z = 0, \tag{1.1}$$

subject to the initial conditions,

$$u(x, y, z, 0) = u_0(x, y, z), \tag{1.2}$$

where $u \in \mathbb{R}^d$ represents the conserved quantities, and f, g, and h are nonlinear fluxes.

Approximate solutions for this type of problems have been traditionally computed with Godunov schemes, [**God59**]. These evolve the solution of (1.1) –and their one- and two-dimensional counterparts– according to the speed and direction of propagation of the characteristic waves of the system. While upwind schemes require a Riemann solver to identify these directions and speeds at cell interfaces, central schemes integrate the solution over staggered cells, resulting in *black-box* type solvers which avoid the costly computation of the characteristic decomposition of the Jacobian matrices of f, g, and h.

1991 *Mathematics Subject Classification.* 65M10, 65M05.

Key words and phrases. Central schemes, hyperbolic conservation laws, non-oscillatory reconstruction.

©0000 (copyright holder)

The paper is structured as follows:

In §2, we provide a full discretisation (in time and space) of (1.1) that allows us to evolve its solution over a staggered grid, essentially an extension of the celebrated one-dimensional Nessayahu-Tadmor central scheme, [**NT90**], and its two dimensional extension by Jiang and Tadmor, [**JT98**]. From the fully-discrete formulation, following the modified central staggered evolution and reprojection approach introduced by Kurganov and Tadmor in [**KT00**], and its two-dimensional extension by Kurganov and Petrova, [**KP01**], we arrive at a genuenly three-dimensional, non-staggered, central semi-discrete formulation for (1.1). In §3, we discuss the various options for the actual implementation of this more versatile semi-discrete formulation. The performance of the proposed scheme is validated in §4, where we present the simulation of the interaction of a gas cloud with a shock wave.

2. Semi-discrete Central Formulation for 3D Conservation Laws

In this section we outline the derivation of a semi-discrete central formulation for the hyperbolic conservation law (1.1). We first introduce a fully-discrete, staggered central formulation for approximating the solutions of the conservation law. This formulation leads to a family of *black-box* type numerical schemes, and serves as the building block of the semi-discrete formulation that we seek.

2.1. Fully-discrete Formulation. As in the 1D and 2D cases, the semi-discrete formulation we seek for 3D conservation laws follows from a fully-discrete central *staggered* discretization of (1.1). First, we fix spatial scales Δx, Δy, and Δz, and define the averages of u at time $t = t^n$ over the mesh cell centered at (x_i, y_j, z_k) and size $\Delta x \times \Delta y \times \Delta z$,

$$\overline{u}^n_{i,j,k} := \frac{1}{|\Delta x \Delta y \Delta z|} \int_{x_i - \frac{\Delta x}{2}}^{x_i + \frac{\Delta x}{2}} \int_{y_j - \frac{\Delta y}{2}}^{y_j + \frac{\Delta y}{2}} \int_{z_k - \frac{\Delta z}{2}}^{z_k + \frac{\Delta z}{2}} u(x, y, z, t^n)\, dx\, dy\, dz. \tag{2.1}$$

The conservation law is integrated over the staggered control volume $V_{i+\frac{1}{2},j+\frac{1}{2},k+\frac{1}{2}} \times [t^n, t^n + \Delta t]$, where $V_{i+\frac{1}{2},j+\frac{1}{2},k+\frac{1}{2}}$ denotes the cell centered at $(x_{i+\frac{1}{2}}, y_{j+\frac{1}{2}}, z_{k+\frac{1}{2}})$. Omitting the variables of integration in the flux integrals (*i.e.*, $u_i = u(x_i, y, z, t)$, $u_j = u(x, y_j, z, t)$, etc.) and dropping the subscripts of $V_{i+\frac{1}{2},j+\frac{1}{2},k+\frac{1}{2}}$, for brevity, we obtain an integral equation equivalent to (1.1),

$$\begin{aligned}
\overline{u}^{n+1}_{i+\frac{1}{2}.j+\frac{1}{2},k+\frac{1}{2}} \quad = \quad & \overline{u}^n_{i+\frac{1}{2}.j+\frac{1}{2},k+\frac{1}{2}} \\
& -\frac{1}{|V|}\left[\int_{y_j}^{y_{j+1}} \int_{z_k}^{z_{k+1}} \int_{t^n}^{t^n+\Delta t} (f(u_{i+1}) - f(u_i))\, dt\, dz\, dy \right. \\
& \quad + \int_{x_i}^{x_{i+1}} \int_{z_k}^{z_{k+1}} \int_{t^n}^{t^n+\Delta t} (g(u_{j+1}) - g(u_j))\, dt\, dz\, dx \\
& \quad \left. + \int_{x_i}^{x_{i+1}} \int_{y_j}^{y_{j+1}} \int_{t^n}^{t^n+\Delta t} (h(u_{k+1}) - h(u_k))\, dt\, dy\, dx \right].
\end{aligned} \tag{2.2}$$

In order to obtain a full discretization of this integral equation, we proceed in two steps: First, we compute $\overline{u}^n_{i+\frac{1}{2},j+\frac{1}{2},k+\frac{1}{2}}$ by averaging over the staggered cells $V_{i+\frac{1}{2},j+\frac{1}{2},k+\frac{1}{2}}$ a piecewise non-oscillatory polynomial $R(x,y,z;\overline{u}^n)$ that interpolates the point values of $u(x,y,z,t^n)$ in each cell $V_{i,j,k}$,

$$R(x,y,z;\overline{u}^n) = \sum_i \sum_j \sum_k p^n_{i,j,k}(x,y,z) \cdot \mathbf{1}_{V_{i,j,k}}(x,y,z). \tag{2.3}$$

That is, letting $V_{q,r,s} = V_{i+\frac{1}{2},j+\frac{1}{2},k+\frac{1}{2}} \cap V_{i+q,j+r,k+s}$ for $q,r,s = 0,1$, the staggered cell averages are given by

$$\overline{u}^n_{i+\frac{1}{2},j+\frac{1}{2},k+\frac{1}{2}} := \frac{1}{|V|} \sum_{q=0}^{1} \sum_{r=0}^{1} \sum_{s=0}^{1} \iiint_{V_{q,r,s}} p^n_{i+q,j+r,k+s}(x,y,z)\, dV. \tag{2.4}$$

Second, we note that under the appropriate CFL conditions the fluxes f, g, and h remain smooth over the staggered cells, so that the three interface flux integrals on the right hand side of (2.2) can be approximated with simple quadrature rules (*e.g.*, midpoint, Simpson's, Gaussian quadrature, etc.) both in space and time. Denoting these approximations respectively by the differences $\mathcal{F}^{n+\frac{1}{2}}_{i+1,j,k} - \mathcal{F}^{n+\frac{1}{2}}_{i,j,k}$, $\mathcal{G}^{n+\frac{1}{2}}_{i,j+1,k} - \mathcal{G}^{n+\frac{1}{2}}_{i,j,k}$, and $\mathcal{H}^{n+\frac{1}{2}}_{i,j,k+1} - \mathcal{H}^{n+\frac{1}{2}}_{i,j,k}$, results in the 3D NT type predictor-corrector formulation:

$$u^{n+\frac{1}{2}}_{i,j,k} = \overline{u}^n_{i,j,k} - \frac{\lambda}{2}(f_x)_{i,j,k} - \frac{\mu}{2}(g_y)_{i,j,k} - \frac{\eta}{2}(h_z)_{i,j,k} \tag{2.5}$$

where $\lambda = \frac{\Delta x}{\Delta t}$, $\mu = \frac{\Delta y}{\Delta t}$, and $\eta = \frac{\Delta z}{\Delta t}$, and the symbols $(f_x)_{i,j,k}$, $(g_y)_{i,j,k}$, and $(h_z)_{i,j,k}$ stand for suitable non-oscillatory numerical derivatives of the flux functions; followed by

$$\begin{aligned} \overline{u}^{n+1}_{i+\frac{1}{2},j+\frac{1}{2},k+\frac{1}{2}} &= \overline{u}^n_{i+\frac{1}{2},j+\frac{1}{2},k+\frac{1}{2}} - \lambda \left[\mathcal{F}^{n+\frac{1}{2}}_{i+1,j,k} - \mathcal{F}^{n+\frac{1}{2}}_{i,j,k} \right] \\ &\quad - \mu \left[\mathcal{G}^{n+\frac{1}{2}}_{i,j+1,k} - \mathcal{G}^{n+\frac{1}{2}}_{i,j,k} \right] - \eta \left[\mathcal{H}^{n+\frac{1}{2}}_{i,j,k+1} - \mathcal{H}^{n+\frac{1}{2}}_{i,j,k} \right]. \end{aligned} \tag{2.6}$$

In essence, the implementation of the predictor-corrector scheme (2.5) - (2.6) requires two main ingredients: # 1 a non-oscillatory reconstruction to recover the staggered cell averages $\overline{u}^n_{i+\frac{1}{2},j+\frac{1}{2},k+\frac{1}{2}}$ from the cell averages $\overline{u}^n_{i+q,j+r,k+s}$, $(q,r,s,= 0,1)$, and # 2 an appropriate combination of quadrature rules for the spatial and temporal flux integrals, including an appropriate time evolution routine to calculate the intermediate time values $u^{n+\beta}$ as required by the quadrature rule used for time integration.

2.2. Modified Staggering. While robust and simple, the schemes resulting from (2.5) - (2.6) still require the calculation of a considerable number of staggered cell averages, numerical derivatives, flux integrals and approximations of u at intermediate time values, making their implementation impractical. Following [**KT00**] and [**KP01**], we introduce the information provided by the maximum speed of

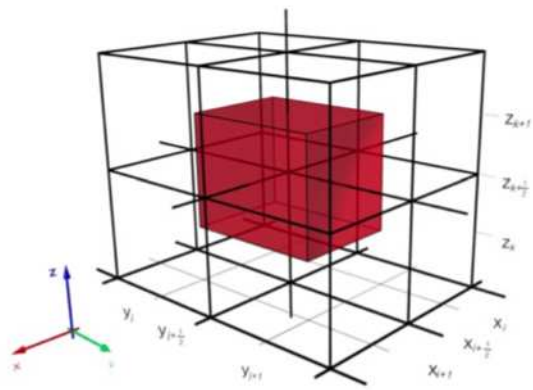

Figure 2.1: Staggered central mesh for 3D scheme: staggered cell average over the dark cell, $\overline{u}^{n+1}_{i+\frac{1}{2},j+\frac{1}{2},k+\frac{1}{2}}$, evolved from the cell averages $\overline{u}^{n}_{i,j,k}$ –clear cells.

propagation across the cell interfaces $x_{i\pm\frac{1}{2}}$, $y_{j\pm\frac{1}{2}}$, and $z_{k\pm\frac{1}{2}}$,

$$
\begin{aligned}
a^x_{i\pm\frac{1}{2},j,k} &= \max_{u\in\mathcal{S}^x_{i\pm\frac{1}{2}}} \rho\left(\frac{\partial f}{\partial u}(u)\right)\\
a^y_{i,j\pm\frac{1}{2},k} &= \max_{u\in\mathcal{S}^y_{j\pm\frac{1}{2}}} \rho\left(\frac{\partial g}{\partial u}(u)\right)\\
a^z_{i,j,k\pm\frac{1}{2}} &= \max_{u\in\mathcal{S}^z_{k\pm\frac{1}{2}}} \rho\left(\frac{\partial h}{\partial u}(u)\right),
\end{aligned}
\tag{2.7}
$$

where $\rho(A)$ denotes the spectral radius of A, and $\mathcal{S}^{x,y,z}$ stands for the surface connecting the two states of the solution across the corresponding interface.

These allow us to differentiate the regions within each mesh cell where the solution of (1.1) remains smooth from those where discontinuities propagate in one or more directions (see figure 2.2), and calculate four different sets of staggered solutions within these smaller regions:

(1) At the cell corners discontinuities propagate in all three directions. There, we calculate (eight) solutions $\overline{w}^{n+1}_{i\pm\frac{1}{2},j\pm\frac{1}{2},k\pm\frac{1}{2}}$ over the *reduced* staggered cells centered at $(x_{i\pm\frac{1}{2}}, y_{j\pm\frac{1}{2}}, z_{k\pm\frac{1}{2}})$ of size $\left(\prod_{s=x,y,z}\mathcal{A}^s_{i\pm\frac{1}{2},j\pm\frac{1}{2},k\pm\frac{1}{2}}\right)(\Delta t)^3$, where, for instance, $\mathcal{A}^x_{i+\frac{1}{2},j\pm\frac{1}{2},k\pm\frac{1}{2}} := \max_{\pm}\{a_{i+\frac{1}{2},j\pm\frac{1}{2},k\pm\frac{1}{2}}\}$ stands for the maximum speed of propagation in the x direction at that cell corner $(x_{i+\frac{1}{2}}, y_{j+\frac{1}{2}}, z_{k+\frac{1}{2}})$, figure 2.2(a).

(2) Along the edges of the original cell, discontinuities propagate in two directions. Three sets of solutions (twelve total) are calculated there: $\overline{w}^{n+1}_{i\pm\frac{1}{2},j\pm\frac{1}{2},k}$, $\overline{w}^{n+1}_{i\pm\frac{1}{2},j,k\pm\frac{1}{2}}$, and $\overline{w}^{n+1}_{i,j\pm\frac{1}{2},k\pm\frac{1}{2}}$. The size of these cells along the edges are of order $(\Delta t)^2$, figure 2.2(b).

(3) Across the faces of the original cell, $x_{i\pm\frac{1}{2}}$, $y_{j\pm\frac{1}{2}}$, and $z_{k\pm\frac{1}{2}}$, six more solutions are calculated: $\overline{w}^{n+1}_{i\pm\frac{1}{2},j,k}$, $\overline{w}^{n+1}_{i,j\pm\frac{1}{2},k}$, and $\overline{w}^{n+1}_{i,j,k\pm\frac{1}{2}}$. In this case, the size of the staggered cells is of order Δt, figure 2.2(c).

(4) Within the interior of the cell, $D_{i,j,k}$, where the solution remains smooth, we simply integrate the conservation law and obtain $\overline{w}^{n+1}_{i,j,k}$, figure 2.2(d).

These 27 solutions are then reprojected onto the original mesh so as to recover the non-staggered cell averages of u at time $t = t^{n+1}$. To this end, we first calculate a non-oscillatory polynomial,

$$\begin{aligned}\widetilde{w}^{n+1}_{i,j,k}(x,y,z) := \sum_{i,j,k} \Big(& \widetilde{w}^{n+1}_{i,j,k}\,\widetilde{\chi}_{i,j,k} + \widetilde{w}^{n+1}_{i+\frac{1}{2},j,k}\,\widetilde{\chi}_{i+\frac{1}{2},j,k} + \widetilde{w}^{n+1}_{i,j+\frac{1}{2},k}\,\widetilde{\chi}_{i,j+\frac{1}{2},k} \\ & + \widetilde{w}^{n+1}_{i,j,k+\frac{1}{2}}\widetilde{\chi}_{i,j,k+\frac{1}{2}} + \widetilde{w}^{n+1}_{i+\frac{1}{2},i+\frac{1}{2},k}\widetilde{\chi}_{i+\frac{1}{2},j+\frac{1}{2},k} + \widetilde{w}^{n+1}_{i+\frac{1}{2},j,k+\frac{1}{2}}\widetilde{\chi}_{i+\frac{1}{2},j,k+\frac{1}{2}} \\ & + \widetilde{w}^{n+1}_{i,j+\frac{1}{2},k+\frac{1}{2}}\widetilde{\chi}_{i,j+\frac{1}{2},k+\frac{1}{2}} + \widetilde{w}^{n+1}_{i+\frac{1}{2},j+\frac{1}{2},k+\frac{1}{2}}\widetilde{\chi}_{i+\frac{1}{2},j+\frac{1}{2},k+\frac{1}{2}} \Big),\end{aligned} \tag{2.8}$$

in order to approximate $u(x,y,z,t^{n+1})$; where each of the polynomial pieces on the write interpolate the corresponding cell average, $\overline{w}^{n+1}$, described above. This polynomial is then averaged over the original grid to obtain the new cell averages,

$$\overline{u}^{n+1}_{i,j,k} = \frac{1}{|\Delta x \Delta y \Delta z|} \int_{x_i-\frac{\Delta x}{2}}^{x_i+\frac{\Delta x}{2}} \int_{y_j-\frac{\Delta y}{2}}^{y_j+\frac{\Delta y}{2}} \int_{z_k-\frac{\Delta z}{2}}^{z_k+\frac{\Delta z}{2}} \widetilde{w}^{n+1}_{i,j,k}(x,y,z)\,dx\,dy\,dz. \tag{2.9}$$

This process, originally introduced for 1D conservation laws in [**JLL+98**], renders a new family of non-staggered fully-discrete central schemes. In higher space dimensions, however, has no practical use as the number of non-smooth solutions to interpolate and reproject makes it implementation overly complicated.

Instead, we only consider these collection of smooth and non-smooth solutions and the reprojected cell averages $\overline{u}^{n+1}_{i,j,k}$ formally, and investigate their asymptotic expansions as we evaluate the limit

$$\frac{d}{dt}\overline{u}_{i,j,k}(t) := \lim_{\Delta t\to 0} \frac{\overline{u}_{i,j,k}(t^n+\Delta t) - \overline{u}_{i,j,k}(t^n)}{\Delta t} \tag{2.10}$$

to obtain a consisitent discretization of the time derivative of the cell averages.

2.3. The Semi-discrete Limit. In order to evaluate the limit (2.10), we re-write it in terms of the interpolating polynomial (2.3)

$$\frac{d}{dt}\overline{u}_{i,j,k}(t) = \lim_{\Delta t\to 0} \frac{1}{\Delta t}\left[\frac{1}{|V|}\int_{x_{i-\frac{1}{2}}}^{x_{i+\frac{1}{2}}} \int_{y_{j-\frac{1}{2}}}^{y_{j+\frac{1}{2}}} \int_{z_{k-\frac{1}{2}}}^{z_{k+\frac{1}{2}}} \widetilde{w}^{n+1}\,dz\,dy\,dx - \overline{u}^n_{i,j,k}\right], \tag{2.11}$$

and observe that

$$\widetilde{w}^{n+1}_{i\pm\frac{1}{2},j\pm\frac{1}{2},k\pm\frac{1}{2}}(x,y,z) = \overline{w}^{n+1}_{i\pm\frac{1}{2},j\pm\frac{1}{2},k\pm\frac{1}{2}} + \mathcal{O}((\Delta t)^3) \tag{2.12a}$$

$$\widetilde{w}^{n+1}_{i\pm\frac{1}{2},j\pm\frac{1}{2},k}(x,y,z) = \overline{w}^{n+1}_{i+\frac{1}{2},j+\frac{1}{2},k} + \mathcal{O}((\Delta t)^2) \tag{2.12b}$$

$$\widetilde{w}^{n+1}_{i\pm\frac{1}{2},j,k}(x,y,z) = \overline{w}^{n+1}_{i\pm\frac{1}{2},j,k} + \mathcal{O}(\Delta t). \tag{2.12c}$$

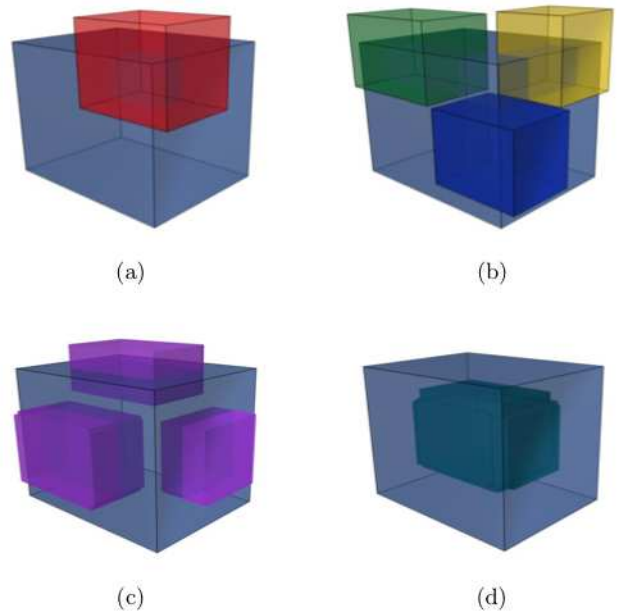

Figure 2.2: Modified staggered evolution: (a) corner cell averages, (b) edges cell averages, (c) cell interface cell averages, and (d) where solution remains smooth in the interior of the cell.

This implies that the contributions from the staggered solution at the cell corners, $\overline{w}^{n+1}_{i\pm\frac{1}{2},j\pm\frac{1}{2},k\pm\frac{1}{2}}$, and cell edges, $\overline{w}^{n+1}_{i\pm\frac{1}{2},j\pm\frac{1}{2},k}$, $\overline{w}^{n+1}_{i\pm\frac{1}{2},j,k\pm\frac{1}{2}}$ and $\overline{w}^{n+1}_{i,j\pm\frac{1}{2},k\pm\frac{1}{2}}$, vanish in the limit $\Delta t \to 0$, so (2.11) reduces to

$$\frac{d}{dt}\overline{u}_{i,j,k} = \lim_{\Delta t\to 0}\frac{1}{\Delta t\,\Delta x\Delta y\Delta z}\Big[\sum_{\pm}\iiint_{S_{i\pm\frac{1}{2},j,k}}\overline{w}^{n+1}_{i\pm\frac{1}{2},j,k}dx\,dy\,dz \tag{2.13}$$

$$+\sum_{\pm}\iiint_{S_{i,j\pm\frac{1}{2},k}}\overline{w}^{n+1}_{i,j\pm\frac{1}{2},k}dx\,dy\,dz+\sum_{\pm}\iiint_{S_{i,j,k\pm\frac{1}{2}}}\overline{w}^{n+1}_{i,j,k\pm\frac{1}{2}}dx\,dy\,dz\Big]$$

$$+\lim_{\Delta t\to 0}\frac{1}{\Delta t}\left[\frac{|D_{i,j,k}|}{\Delta x\Delta y\Delta t}\overline{w}^{n+1}_{i,j,k}-\overline{u}^{n}_{i,j,k}\right],$$

where $S^x_{i\pm\frac{1}{2},j,k}$, $S^y_{i,j\pm\frac{1}{2},k}$, $S^z_{i,j,k\pm\frac{1}{2}}$ represent the cell interfaces of the original cell, and $D_{i,j,k}$ its interior, where the solution remains smooth. The three sums on the right hand side amount, respectively, to

$$\frac{a^x_{i+\frac{1}{2},j,k}}{\Delta x}\lim_{\Delta t\to 0}\overline{w}^{n+1}_{i+\frac{1}{2},j,k},\quad \frac{a^y_{i,j\pm\frac{1}{2},k}}{\Delta y}\lim_{\Delta t\to 0}\overline{w}^{n+1}_{i,j\pm\frac{1}{2},k},\quad \frac{a^z_{i,j,k\pm\frac{1}{2}}}{\Delta z}\lim_{\Delta t\to 0}\overline{w}^{n+1}_{i,j,k\pm\frac{1}{2}} \tag{2.14}$$

and the second limit, involving the smooth solution, $\overline{w}^{n+1}_{i,j,k}$, amounts to the cell average $\overline{u}^{n}_{i,j,k}$ minus the integral of u along the edges of the cell, [**KP01**].

Finally, we notice that he limits in (2.14) reduce to double integrals (along two space dimensions each) that can be approximated with iterated quadrature rules, rendering the semi-discrete formulation

$$\frac{d}{dt}\overline{u}_{i,j,k} = -\frac{1}{\Delta x}\left[H^x_{i+\frac{1}{2},j,k} - H^x_{i-\frac{1}{2},j,k}\right] - \frac{1}{\Delta y}\left[H^y_{i,j+\frac{1}{2},k} - H^y_{i,j-\frac{1}{2},k}\right] - \frac{1}{\Delta z}\left[H^z_{i,j,k+\frac{1}{2}} - H^z_{i,j,k-\frac{1}{2}}\right], \tag{2.15}$$

where the exact expression of numerical fluxes, $H^x_{i\pm\frac{1}{2},j,k}$, $H^y_{i,j,k\pm\frac{1}{2}}$, $H^z_{i,j\pm\frac{1}{2},k}$ will depend on the quadrature rule chosen; for our present discussion, we chose the midpoint rule, which renders:

$$H^x_{i+\frac{1}{2}} = \frac{1}{2}\left[f(u^{\mathrm{W}}_{i+1,j,k}) + f(u^{\mathrm{E}}_{i,j,k})\right] - \frac{a^x_{i+\frac{1}{2},j,k}}{2}\left[u^{\mathrm{W}}_{i+1,j,k} - u^{\mathrm{E}}_{i,j,k}\right], \tag{2.16}$$

where, $u^{\mathrm{E}}_{i,j,k}$ and $u^{\mathrm{W}}_{i+\frac{1}{2},j,k}$ represent interface point values of u at each side of the cell interface $x_{i+\frac{1}{2}}$, reconstructed from the original cell averages $\overline{u}^n_{i,j,k}$. Similar point values need to be recovered along the y direction, $u^{\mathrm{N}}_{i,j,k}$ and $u^{\mathrm{S}}_{i,j+\frac{1}{2},k}$, and z direction, $u^{\mathrm{T}}_{i,j,k+\frac{1}{2}}$ and $u^{\mathrm{B}}_{i,j,k}$, in order to compute the corresponding fluxes $H^y_{i,j,k\pm\frac{1}{2}}$, and $H^z_{i,j\pm\frac{1}{2},k}$.

3. Implementation of Multidimensional Central Schemes

The actual implementation of the semi-discrete central formulation (2.15) requires two main ingredients for its implementation as a numerical scheme: #1 a piecewise non-oscillatory polynomial reconstruction like that required for the fully-discrete formulation, (2.3), and #2 an evolution routine to solve the resulting system of ODEs.

3.1. Polynomial Reconstruction. The reconstruction procedure is at the heart of high-resolution, non-oscillatory central schemes, and requires the coefficients of the polynomials on the right of (2.3) to be determined so that the following three essential properties are satisfied:

- $\mathcal{P}_1$ — Conservation of cell averages: $\overline{p}_{i,j,k}(x,y,z) = \overline{u}^n_{i,j,k}$.
- $\mathcal{P}_2$ — Accuracy: $R(x,y,z;\overline{w}^{n+1}) = u(x,y,z,t) + \mathcal{O}((\Delta x)^r)$ for r^{th}-order accurate scheme, wherever $u(x,y,z,t)$ is sufficiently smooth.
- $\mathcal{P}_3$ — Non-oscillatory behavior.

3.2. Non-oscillatory Second-order Reconstruction. For the example presented below, we chose the polynomials

$$p_j(x) = \overline{u}_j + (u_x)_{i,j,k}(x - x_i) + (u_y)_{i,j,k}(y - y_j) + (u_z)_{i,j,k}(z - z_k) \tag{3.1}$$

with the slopes $(u_s)_{i,j,k}$, $s = x, y, z$, given by the limiter, [**vL97, Har83**],

$$(u_s)_{i,j,k} = \frac{1}{\Delta s}\mathrm{MinMod}\left(\alpha\Delta^s_-\overline{u}_{i,j,k},\ \Delta^s_0\overline{u}_{i,jk},\ \alpha\Delta^s_+\overline{u}_{i,j,k}\right), \tag{3.2}$$

where $1 \leq \alpha < 2$, $\Delta^s_{-/o/+}$ stands for the first order backward/centered/forward difference operator in the s direction, and

$$\text{MinMod}(x_1, x_2, x_3, \ldots, x_k) = \begin{cases} \min_j(x_j) & \text{if} \quad x_j > 0 \quad \forall\, j \\ \max_j(x_j) & \text{if} \quad x_j < 0 \quad \forall\, j \\ 0 & \text{otherwise} \end{cases} . \tag{3.3}$$

Other non-oscillatory reconstruction procedures such as third-order dimension-by-dimension Central WENO reconstructions, [**LPR99**], have been tested within the scope of this work.

3.3. Time Evolution: SSP Runge-Kutta Solvers. Once equipped with the reconstructed interface values from the cell average of the solution at time t^n as described in §3.2, we need an evolution routine to approximate the solution of the ODEs at time $t^n + \Delta t$ according to (2.15). To this end, we choose the second order *Strong Stability Preserving* Runge-Kutta scheme, [**SO89, GST01**],

$$\begin{aligned} u^{(1)} &= u^{(0)} \quad + \quad \Delta t\, C[u^{(0)}], \\ \overline{u}^{n+1} &= u^{(1)} \quad + \quad \frac{\Delta t}{2}(C[u^{(1)}] + C[u^{(0)}]), \end{aligned} \tag{3.4}$$

with

$$\begin{aligned} C[u] \quad = \quad & -\frac{H^x_{i+\frac{1}{2},j,k}(u) - H^x_{i-\frac{1}{2},j,k}(u)}{\Delta x} \\ & -\frac{H^y_{i,j+\frac{1}{2},k}(u) - H^y_{i,j-\frac{1}{2},k}(u)}{\Delta y} - \frac{H^z_{i,j,k+\frac{1}{2}}(u) - H^z_{i,j,k-\frac{1}{2}}(u)}{\Delta z}. \end{aligned} \tag{3.5}$$

4. Numerical Test

In order to test the ability of the proposed scheme to approximate the solution of hyperbolic conservation law, we solve Euler equations of gas dynamics, which we write in the form (1.1) with

$$\begin{aligned} u &= \big(\rho,\ \rho v_x,\ \rho v_y,\ \rho v_z,\ E\big)^\top, \\ f(u) &= \big(\rho v_x,\ \rho v_x^2 + p,\ \rho v_x v_y,\ \rho v_x v_z,\ (E+p)v_x\big)^\top, \\ g(u) &= \big(\rho v_y,\ \rho v_x v_y,\ \rho v_y^2 + p,\ \rho v_y v_z,\ (E+p)v_y\big)^\top, \\ h(u) &= \big(\rho v_z,\ \rho v_x v_z,\ \rho v_y v_z,\ \rho v_z^2 + p,\ (E+p)v_z\big)^\top, \end{aligned} \tag{4.1}$$

and equation of state

$$p = (\gamma - 1)\left(E - \frac{1}{2}\rho\,(v_x^2 + v_y^2 + v_z^2)\right).$$

In particular, we simulate the interaction of a low density gas bubble of radius, $r = 0.2$, centered at $(0.5, 0, 0)$ with a shock wave, [**LLB$^+$08**]. The shock is initially at $x = 0.2$, and the initial conditions to the right of the shock and outside the bubble are given by,

$$(\rho, u, v, w, p)^\top = (1, 0, 0, 0, 1)^\top;$$

inside the bubble the pressure and density are $p = 1$ and $\rho = 0.1$, and to the left of the shock, they are determined by the Rankine-Hugoniot conditions, [**LeV92**]. The problem is solved in the first quadrant on a $240 \times 80 \times 80$ mesh, using reflective boundary conditions along the right y boundary and bottom z boundary, and free flow conditions elsewhere. We evolve the solution until the shock passes (and sweeps) the bubble, t = 0.3, see figure 4 below.

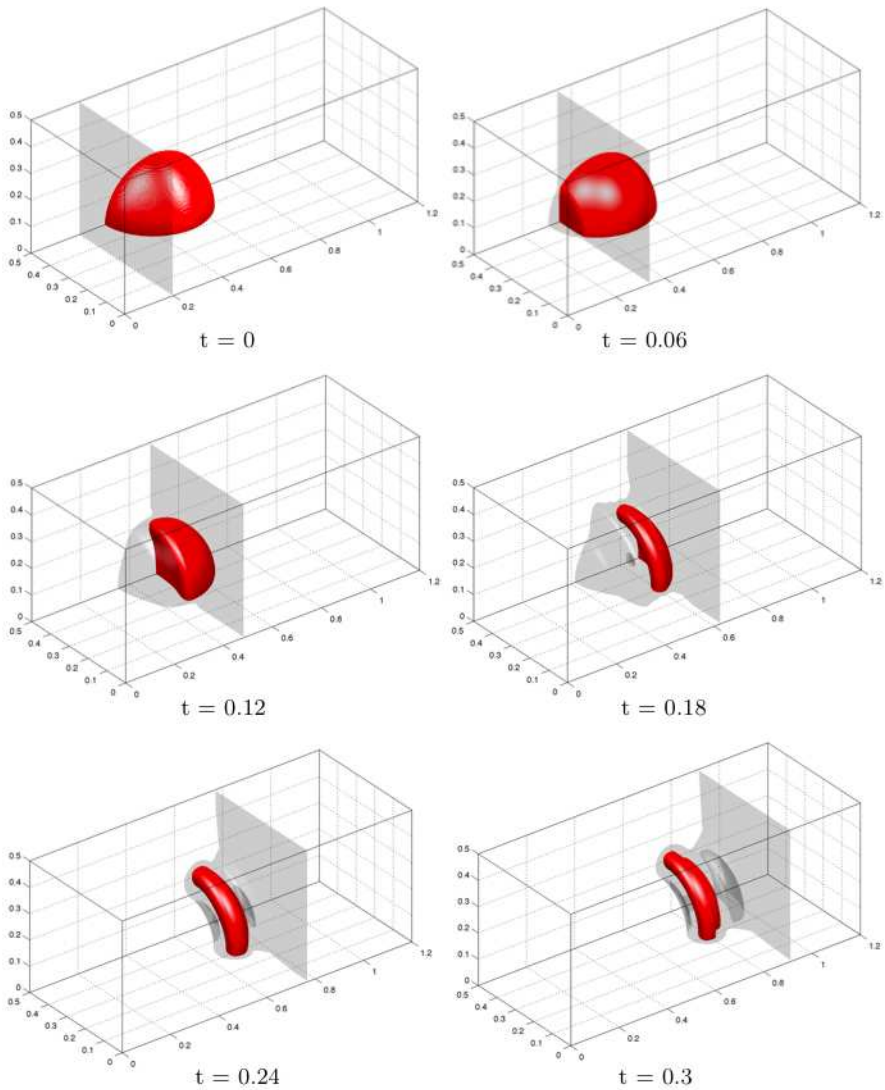

Figure 4.1: Interaction of gas cloud and shock wave at various times, isosurfaces of gas density, red $\rho = 0.5$, grey $\rho = 2.4$.

These results demonstrate the robustness and stability of the proposed central scheme to evolve the solution of hyperbolic conservation laws. For additional results and details, consult [**BT06**].

References

[BT06] Jorge Balbás and Eitan Tadmor, CentPack, Available for download at http://www.cscamm.umd.edu/centpack/, July 2006.

[God59] S. K. Godunov, *A difference method for numerical calculation of discontinuous solutions of the equations of hydrodynamics*, Mat. Sb. (N.S.) **47 (89)** (1959), 271–306. MR MR0119433 (22 #10194)

[GST01] Sigal Gottlieb, Chi-Wang Shu, and Eitan Tadmor, *Strong stability-preserving high-order time discretization methods*, SIAM Rev. **43** (2001), no. 1, 89–112 (electronic). MR 2002f:65132

[Har83] Amiram Harten, *High resolution schemes for hyperbolic conservation laws*, J. Comput. Phys. **49** (1983), 357–393. MR 85h:65188

[JLL+98] G.-S. Jiang, D. Levy, C.-T. Lin, S. Osher, and E. Tadmor, *High-resolution nonoscillatory central schemes with nonstaggered grids for hyperbolic conservation laws*, SIAM J. Numer. Anal. **35** (1998), no. 6, 2147–2168 (electronic). MR 99j:65145

[JT98] Guang-Shan Jiang and Eitan Tadmor, *Nonoscillatory central schemes for multidimensional hyperbolic conservation laws*, SIAM J. Sci. Comput. **19** (1998), no. 6, 1892–1917 (electronic). MR 99f:65128

[KP01] Alexander Kurganov and Guergana Petrova, *A third-order semi-discrete genuinely multidimensional central scheme for hyperbolic conservation laws and related problems*, Numer. Math. **88** (2001), no. 4, 683–729. MR 2002e:65118

[KT00] Alexander Kurganov and Eitan Tadmor, *New high-resolution central schemes for nonlinear conservation laws and convection-diffusion equations*, J. Comput. Phys. **160** (2000), no. 1, 241–282. MR 2001d:65135

[LeV92] Randall J. LeVeque, *Numerical methods for conservation laws*, second ed., Lectures in Mathematics ETH Zürich, Birkhäuser Verlag, Basel, 1992. MR MR1153252 (92m:65106)

[LLB+08] Randall J. LeVeque, Jan Olav Langseth, Marsha Berger, David McQueen, Donna Calhoun, Peter Blossey, and Sorin Mitran, clawpack, Available for download at http://www.amath.washington.edu/∼claw/, 2008.

[LPR99] Doron Levy, Gabriella Puppo, and Giovanni Russo, *Central WENO schemes for hyperbolic systems of conservation laws*, M2AN Math. Model. Numer. Anal. **33** (1999), no. 3, 547–571. MR 2000f:65079

[NT90] Haim Nessyahu and Eitan Tadmor, *Nonoscillatory central differencing for hyperbolic conservation laws*, J. Comput. Phys. **87** (1990), no. 2, 408–463. MR 91i:65157

[SO89] Chi-Wang Shu and Stanley Osher, *Efficient implementation of essentially nonoscillatory shock-capturing schemes. II*, J. Comput. Phys. **83** (1989), no. 1, 32–78. MR 90i:65167

[vL97] Bram van Leer, *Towards the ultimate conservative difference scheme. V. A second-order sequel to Godunov's method [J. Comput. Phys.* **32** *(1979), no. 1, 101–136]*, J. Comput. Phys. **135** (1997), no. 2, 227–248. MR 1 486 274

California State University, Northridge, CA 90066, USA
E-mail address: jorge.balbas@csun.edu

University of New Hampshire, Durham, NH 03824, USA
E-mail address: xqian@unh.edu